

Title	First-Principles Calculations of Structure and Magneto-Electric Properties of Co-Doped Bismuth Ferrite
Author(s)	Ricinski, Dan
Citation	サイバーメディアHPCジャーナル. 2012, 2, p. 37-42
Version Type	VoR
URL	https://doi.org/10.18910/70456
rights	
Note	

Osaka University Knowledge Archive : OUKA

<https://ir.library.osaka-u.ac.jp/>

Osaka University

First-Principles Calculations of Structure and Magneto-Electric Properties of Co-Doped Bismuth Ferrite

Dan Ricinski

Tokyo Institute of Technology, Interdisciplinary Graduate School of Science and Engineering

1. Introduction

Among the many multifunctional oxide materials that are discovered and studied nowadays, magnetoelectric multiferroics continue to attract considerable attention in view of applications to multiple-level non-volatile memories and spintronic devices [1]. In particular, a lot of research is focused on bismuth ferrite (BiFeO_3 , BFO), due to its relative ease of fabrication under various structures using modern techniques, as well as its intriguing properties (a rich phase transition portrait due to several competing unit cell instabilities, peculiar coupling between ferroelectricity and antiferromagnetism) [2]. However, while BFO is a ferroelectric with large spontaneous polarization, it is antiferromagnetic (AFM) and therefore its magnetization and magnetoelectric coupling are invariably much smaller than would be useful for applications. Thus one of the issues that still requires a satisfactory solution is the enhancement of its intrinsically-weak BFO magnetism and magneto-electric coupling. To that aim, substitutional A and B-site elements added to the perovskite structure of BFO are believed to be effective [3]. Here we report results of first-principles calculations of BFO doped with Co (BFCO), aiming to enhance its ferroelectric and ferromagnetic properties, as well as the coupling between them.

The selection of Co as B-site doping element in BFO was motivated by the intriguing properties of bismuth cobaltite (BCO) and by the desire to investigate the extent to which they are preserved in the compound resulted from BCO combination with BFO. Specifically, the ground structure of BCO does correspond to a so-called super-tetragonal phase with a giant c/a ratio of

about 1.27 and C-type AFM ordering [4-5], while the stress-relaxed BFO crystal structure has rhombohedral symmetry ($R3c$ space group) and G-type antiferromagnetic (AFM) ordering [6]. The significantly different crystallographic symmetries and magnetic ordering of the ground structure for the two end-members of BFCO suggests an interesting question with respect to what would be the most favourable symmetry and magnetic ordering in the mixed compound. Additionally, a super-tetragonal phase of BFO with a c/a ratio of about 1.26 has been reported as possible in several publications [7-8], making the question of whether or not the multiferroic properties of BFCO are BFO-like, BCO-like or entirely different from BFO and BCO even more intriguing. Indeed, one expects enhanced magnetism and magnetoelectric coupling in BFCO compared to its isolated components, due to the uncompensated spin configurations of the B-site magnetic ion (Fe^{3+} and Co^{3+} , with a nominal magnetic moment of $5\mu_B$ and $4\mu_B$, respectively). Moreover, there are reports of different spin configurations for the Co^{3+} ion in BCO as well as a pressure-induced phase transition from high-spin to nonmagnetic low-spin configuration [9-10]. This raises the prospect of a complex interplay between the crystal symmetries, AFM ordering and local spin configurations in BFCO, which might help making steps towards solving the enduring problem of robust magnetoelectric coupling for materials in the family of BFO. To clarify these aspects, in this paper we analyze the structure and multiferroic properties of various BFCO supercells in which the Fe versus Co composition, crystal symmetry and type of antiferromagnetic ordering are varied.

2. Technical Details of First Principles Calculations

All first-principles calculations have been done using the density functional theory, under the spin-polarized local density approximation including the correction for the strongly correlated 3d electrons of Fe and Co (LDA+U), as implemented in the ABINIT package [11]. For the electronic wavefunctions we used plane-waves truncated at 400 eV, while for all chemical elements we have used projected-augmented wave pseudo-potentials [12]. We have included both valence and semicore states into our calculations, specifically Fe's and Co's 3d and 4s electrons, Bi's 6s and 6p electrons, and O's 2s and 2p electrons. The Brillouin zone integrations were done on a 4x4x4 k-point grid and all structural optimizations were performed until atomic forces are smaller than 2 meV/Å.

3 Results and Discussion

In first step, geometry relaxation of BFO and BCO under various symmetries and AFM configurations has been performed. The lowest energy configuration corresponds to a rhombohedral structure with $R3c$ symmetry (having a lattice constant of 5.54 Å and primitive cell angle of 59.7°) and G-type AFM ordering in case of BFO, and to a super-tetragonal structure with $P4mm$ symmetry (having lattice constants of 3.67 Å and 4.66 Å) and C-type AFM ordering in case of BCO. The calculated lattice parameters, the values of local $\text{Fe}^{3+}/\text{Co}^{3+}$ magnetic moment and the determined ground structures were similar to previous reports of first-principles calculation results [11]. The calculated local magnetic moments for Fe^{3+} and Co^{3+} were within 1 μ_B of the expected values for these ions in an ideal chemical configuration, due to the large Fe-O and Co-O covalency effects.

Using a supercell with four BFO formula units and substituting one of the Fe atoms with Co, we have investigated the energetics, structure and magneto-electric properties of 12.5% Co-doped BFO

(further denoted to as 12BFCO) with various crystal symmetries, as illustrated in Fig. 1.

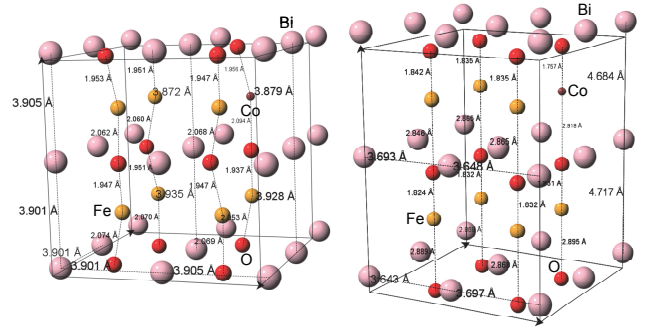


Figure 1: Illustration of 12.5% Co-doped BFCO

supercells with $R3c$ (left) and $P4mm$ symmetry (right)

Upon geometry optimization of various supercells, energy considerations based on the results presented in Fig. 2 allowed us to conclude that the most stable structure has rhombohedral symmetry and G-type AFM ordering (similarly with BFO), which was expected for small Co doping content. Among the tetragonal structures of 12BFCO, the one with C-type AFM ordering is energetically favoured over those having G-type and A-type AFM ordering. On the other hand, Fig. 2 also reveals that in the case of 50% Co doped BFO (50BFCO), the tetragonal structure with C-type AFM ordering becomes energetically favored over the other supercells with tetragonal symmetry, as well as over the BFO-like rhombohedral structure. This phase transition occurs because when we substitute Fe with Co to a larger extent, the resulting alloy naturally tends to acquire more of the properties of BCO rather than those of BFO.

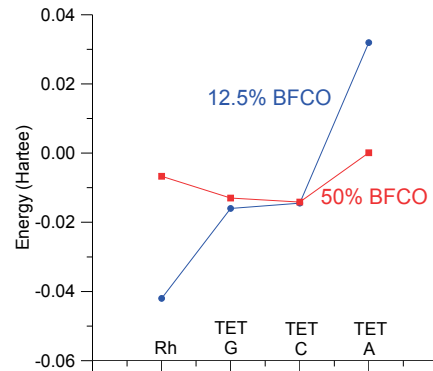


Figure 2: Total energy (referenced to maximum of BFCO50 energy, setting same energy for C-type AFM ordering) of BFCO with various symmetry and Co content

We have further analyzed the structural features of the individual BFO and BCO cells that compose various tetragonal 12BFCO supercells. Specifically, we have examined the spatial distribution of the Fe/Co-O and Bi-O bond length off-centring ratios (this atomic off-centring results from minimizing the total energy/elastic stresses of the supercell during geometry relaxation, yielding a spontaneous polarization) in four perovskite blocks of the tetragonal supercell, as well as the distribution of their tetragonality ratio. The four perovskite blocks selected for analysis are the BCO cell, the BFO cell directly below it, and the diagonally-opposite BFO cells of the above two cells in the upper and lower half of the BFCO12 supercell, respectively (see insets on right of each figure).

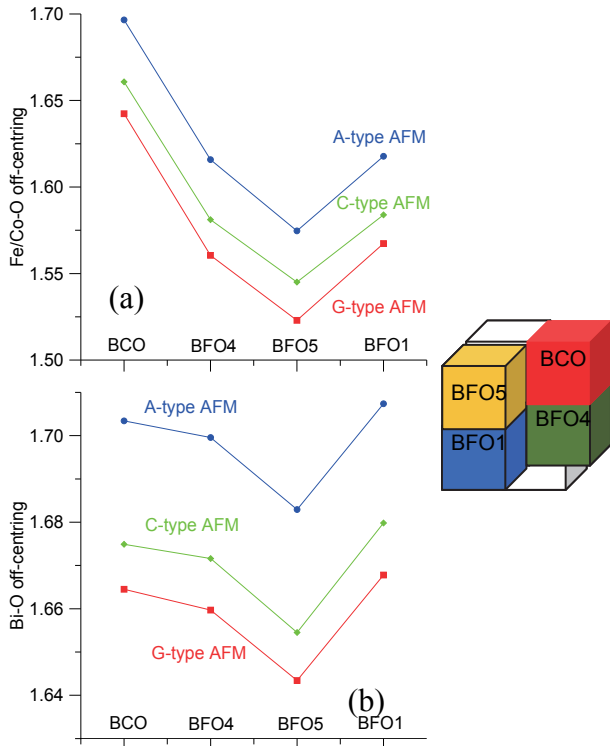


Figure 3: Distribution of Fe/Co-O (a) and Bi-O (b) bond length off-centring ratio in tetragonal BFCO12 supercells

The first important finding is that the magnitude of Bi-O and Fe/Co-O bond length off-centring ratios depends on the type of AFM spin arrangement, while their spatial distribution in the tetragonal BFCO supercell blocks does not. As seen in Figs. 3(a-b), both the Fe/Co-O and Bi-O off-centring ratios are largest in case

of A-type AFM, followed by C-type AFM and followed by G-type AFM. Among the different ABO_3 perovskite blocks, the BCO cell has the largest B-O off-centring, which is to be expected in view of the larger spontaneous polarization calculated by first-principles for BCO, compared to BFO [11]. Interestingly, the smallest Fe-O off-centring was found in the BFO perovskite block diagonally-opposite to BCO in the upper half of the BFCO supercell (further denoted as BFO5), while the two BFO cells directly below BCO (further denoted as BFO4) and diagonally-opposite to it (further denoted as BFO1) in the lower half of the BFCO cell have similar Fe-O off-centring ratio, larger than that of BFO5, but significantly smaller than in BCO. As far as the Bi-O off-centring ratio is concerned, Fig. 3(b) reveals that the smallest value is still found in the BFO5 block, while the largest one occurs in BFO1 block, with BCO having only slightly larger off-centring than BFO4.

Additionally, Figs. 4(a-b) displays the distribution of the tetragonality ratio and spontaneous polarization derived from a point-charge model (using nominal valence charges of Bi^{3+} , Fe^{3+} , Co^{3+} and O^{2-} ions), in tetragonal supercells with various types of AFM ordering. We remark that the spatial distribution of the tetragonality ratio in the BFCO12 supercell (Fig. 4(a)) exhibits similar features with the Bi-O off-centring distribution (Fig. 3(b)), while the spontaneous polarization distribution (Fig. 4(b)) resembles that of the Fe/Co-O off-centring (Fig. 3(a)). However, the tetragonality ratio does not vary significantly when the AFM ordering of the BFCO tetragonal supercell is changed from A-type to C-type, while the G-type AFM ordering continues to provide the smallest c/a from the analyzed tetragonal BFCO12 supercells. On the other hand, the calculation data proves that the spontaneous polarization distribution in the BFCO tetragonal superlattice depends mainly on the Fe/Co off-centring rather than on tetragonality ratio or Bi-O off-centering. Furthermore, an important implication of the

spontaneous polarization dependence on the type of AFM ordering is that in order to enhance the polarization in BFO and related materials, stabilization of usually energetically-unfavourable structures with A-type AFM ordering would be necessary.

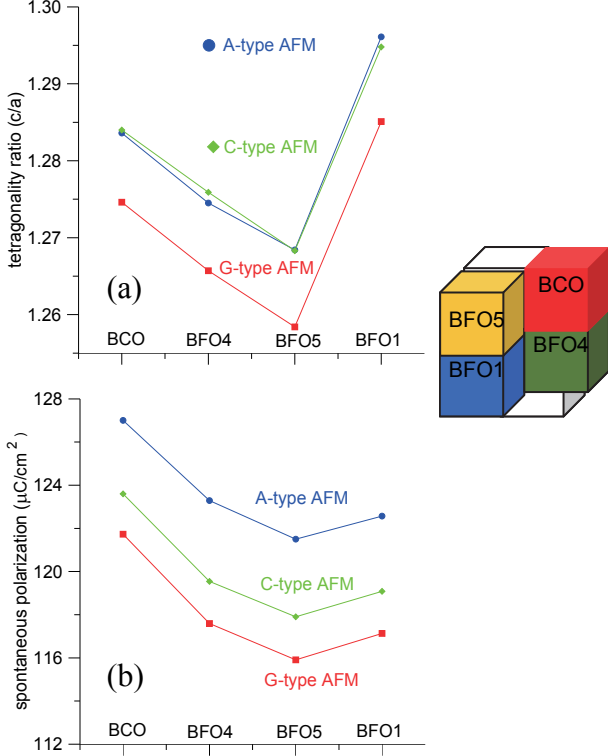


Figure 4: Distribution of tetragonality ratio c/a (a) and spontaneous polarization from point-charge model (b) in tetragonal BFCO12 supercells

The results obtained so far have assumed a high-spin (HS) electronic configuration of the Co atom into the studied BFCO supercells. However, there are previous reports of magnetic moment collapse in BCO under the influence of large external pressures, in which case the Co atom will take on a low-spin (LS) electronic configuration [9-10]. In the case of supercells with mixed BFO-BCO composition, high pressures might be created internally due to structural misfit between the rhombohedral phase of BFO and super-tetragonal phase of BCO in their ground state. Therefore we examined the impact of the Co spin configuration onto the energetics, phase stability, electric/magnetic properties as well as spatial distribution of tetragonality ratio and atomic off-centring in various BFCO supercells.

The calculations have shown that, in contrast to the case of BCO with HS-Co configuration, the rhombohedral structure is the one most energetically-favored among all the supercells with LS-Co that we have analyzed, for both BFCO12 and BFCO50 (Fig. 5). Moreover, since rhombohedral BFCO with a given LS-Co content has a lower total energy than all supercells with equal HS-Co content (irrespective on whether they are rhombohedral or tetragonal), it appears unlikely for the Co atom to ever take a high-spin electronic configuration in BFCO. As mentioned above, this might be a consequence of high internal pressure in BFCO caused by the inherent structural misfit of mixing materials with such dramatically different ground state symmetries and lattice parameters.

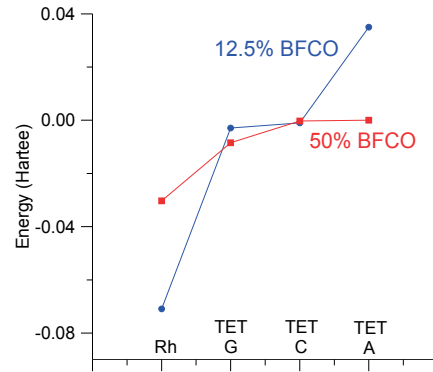


Figure 5: Total energy (referenced to maximum of BFCO50 energy, setting same energy for C-AFM ordering) of BFCO with various symmetry and LS-Co content

The study of atomic off-centring has revealed that the type of AFM ordering has a less significant influence on the magnitude of Fe/Co-O off-centring in Fig. 6(a) (compared to the case of BCO with HS-Co in Fig. 3(a)), while largest Bi-O off-centring is still obtained in case of BFCO12 supercells with A-type AFM ordering, followed by the supercell with C-type AFM ordering and the one with G-type AFM ordering (see Fig. 6(b)).

We have next compared the spatial distribution of A-O and B-O off-centring in ABO_3 blocks of the BFCO12 supercell with HS and LS-Co configurations. We note that in case of LS-Co the BFO4 block exhibits the largest off-centring, while inside BCO blocks the latter is

dramatically reduced, simultaneously with the Co magnetic moment collapse. Further, whereas in case of BFCO12 with HS Co the atomic off-centring increases when passing from the BFO5 to BFO1 block, the perovskite block diagonally-opposite to BCO in the upper half of the BFCO supercell (BFO5) has now larger Bi-O and Fe-O off-centring than those inside BFO1.

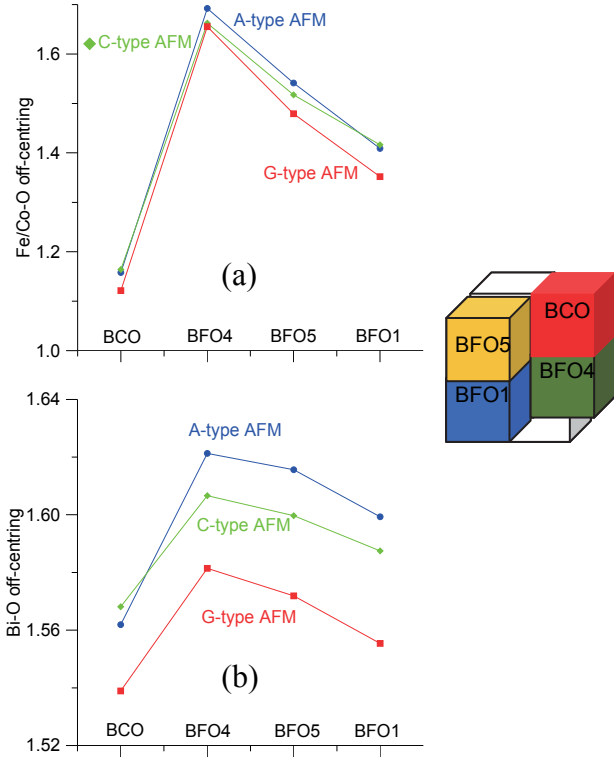


Figure 6: Distribution of Fe/Co-O (a) and Bi-O (b) bond length off-centring ratio in tetragonal BFCO12 supercells with LS-Co

Furthermore, as expected from the previously-reported volume compression induced by the magnetic moment collapse in BCO, the tetragonality ratios of BFCO12 with LS Co are significantly reduced from their giant values calculated in BFCO12 with HS-Co. Particularly, as seen in Fig. 7(a), the BCO perovskite blocks have small c/a ratios irrespective of AFM ordering, while it is only in BFO4 block that the tetragonality ratio has similar values to that of BFO cells inside BFCO12 with HS-Co. (remarkable in this case is also that largest c/a ratio occurs in case of C-type AFM ordering). On the other hand, Fig. 7(b) shows that the spatial distribution of spontaneous polarization derived from the point-charge

model resembles neither that of the Fe/Co-O off-centring, nor that of the Bi-O off-centring.

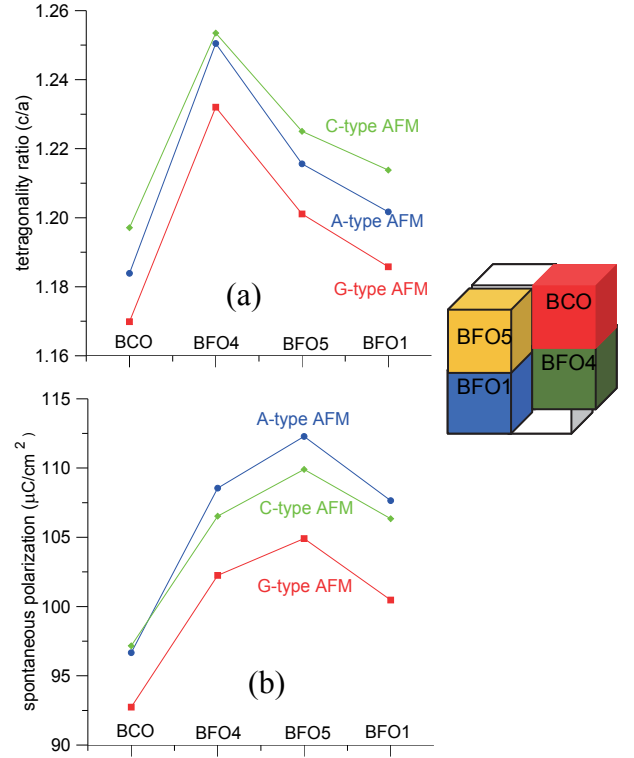


Figure 7: Distribution of tetragonality ratio c/a (a) and spontaneous polarization from point-charge model (b) in tetragonal BFCO12 supercells with LS-Co

Specifically the largest spontaneous polarization was calculated in the BFO5 block (with minimum in the BCO cell), as expected due to the local volume collapse in that cell), which is in fact an exact opposite distribution compared to the case of BFCO12 supercells with HS-Co.

With respect to the magnetoelectric properties, our first-principles calculations revealed that the Co doping can be an effective method to enhance the magnetization of (nominally antiferromagnetic) BFO, from 20 emu/cm^3 in case of 12BFCO (Fig. 8(a)) to 80 emu/cm^3 in case of 50BFCO (Fig. 8(b)). On one hand this was caused by the onset of ferrimagnetic ordering in the BFCO supercells used for calculations, which have incomplete spin compensation due to unequal local magnetic moments at Fe and Co sites. Additionally, while having little influence on the macroscopic magnetization, the type of AFM ordering impacts on the values of the average spontaneous polarization in the supercell, thus proving

that the magnetic and electric interactions in BFCO are intrinsically coupled (the relationship between spontaneous polarization and magnetization of the various supercells can be assessed from Fig. 8). Further, we have shown that the magnetization can be enhanced even more, up to 100 emu/cm^3 in case of 12BFCO and 400 emu/cm^3 in case of 50BFCO, (at the expense of decreasing the tetragonality ratio and the spontaneous polarization) in BFCO supercells where the Co ion takes a low-spin configuration (see Fig. 8).

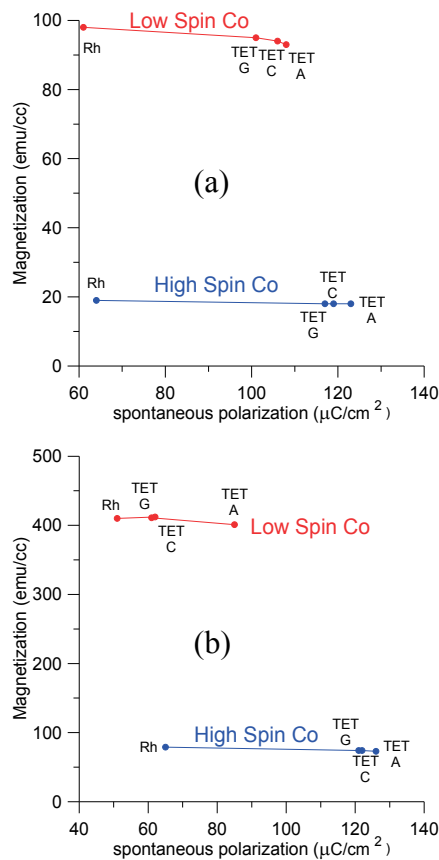


Figure 8: Illustration of magneto-electric coupling in BFCO supercells with various crystal symmetry, AFM ordering, spin configuration for Co ion, for 12.5% Co content (a) and 50% Co content (b)

5. Conclusion

The undertaken first-principles calculations suggest that exploiting the complex interplay between the crystal symmetries, AFM ordering and local spin configurations in Co-doped bismuth ferrite might be helpful in solving the enduring problem of robust magnetoelectric coupling

for materials at room temperature. Specifically, fabricating BFCO thin films where Co is stabilized in a low spin configuration might be a promising method to realize the full potential of these materials. Our results show that a low spin configuration of Co becomes energetically favored in Co-doped BFO and leads to a large magnetization while still maintaining a large polarization (in spite of an overall reduction in tetragonality ratio caused by the local magnetic moment collapse), and therefore it might be the key for achieving the robust magnetoelectric coupling required for the next-generation memory applications.

Acknowledgements

This research was partially supported by the Grants-in-Aid for Scientific Research 21360150 and 24560007 provided by JSPS. All calculations have been done using the HPC system of the Cybermedia Center, Osaka University.

References

- (1) N. A. Spaldin, et al., *Science* **309**, 391, (2005).
- (2) G. Catalan and J. F. Scott, *Adv. Mater.* **209**, 1 (2009).
- (3) J. M. Park, et al., *Jpn. J. Appl. Phys.* **48**, 09KB03, (2009).
- (4) A. A. Belik, et al., *Chem. Mater.* **18** 798, (2006).
- (5) Y. Uratani, et al., *Jpn. J. Appl. Phys.* **44**, 7130, (2005).
- (6) F. Kubel, et al., *Acta Crystallogr.*, **46**, 698, (1990).
- (7) D. Ricinchi, et al., *J. Phys. Condens. Matter* **18**, L97 (2006).
- (8) R. J. Zeches, et al., *Science* **326**, 977 (2009).
- (9) X. Ming, et al., *J. Phys. Condens. Matter* **21**, 295902 (2009).
- (10) K. Oka, et al., *J. Am. Chem. Soc.* **132**, 9438 (2010).
- (11) X. Gonze, et al., *Computer Phys. Comm.* **180**, 2582-2615 (2009).
- (12) M. Torrent, et al., *Comput. Mat. Science* **42**, 337, (2008).
- (13) K. Miura, et al., *Jpn. J. Appl. Phys.* **49**, 09ME07 (2010).